SCIENCE CHINA
Technological Sciences

•Article•

January 2021 Vol.64 No.1: 65–70
https://doi.org/10.1007/s11431-020-1718-4

Highly sensitive glucose sensor based on hierarchical CuO

CHEN Fang, SHAO Bo, ZHAI Wei* & MA XiaoYan

MOE Key Laboratory of Material Physics and Chemistry under Extraordinary Conditions, Northwestern Polytechnical University, Xi'an 710129, China

Received May 29, 2020; accepted September 7, 2020; published online December 7, 2020

The fabrication of high performance CuO based glucose sensors remains a great challenge due to the "trade-off effect" between sensitivity and linear range. In this study, a hierarchical CuO nanostructure with a great number of firecracker-shaped nanorods along the ligament and three-dimensional interconnected nanoporous is obtained by dealloying and post oxidation process of Al-33.3 wt% Cu eutectic alloy ribbons. Because of the precise structural design, not only the number of active sites for glucose electro-oxidation is significantly increased but also the glucose diffusion under high concentration is greatly accelerated, leading to a high sensitivity of 1.18 mA cm^{-2} mM^{-1} and a wider linear range up to 5.53 mM for glucose detection. This work provides a potential approach to design hierarchical nanostructure for other metal oxides with desirable properties for electrocatalytic applications.

hierarchical CuO nanostructure, dealloying, glucose sensor, highly sensitive

Citation: Chen F, Shao B, Zhai W, et al. Highly sensitive glucose sensor based on hierarchical CuO. Sci China Tech Sci, 2021, 64: 65–70, https://doi.org/10.1007/s11431-020-1718-4

1 Introduction

Copper oxide (CuO), a typical nontoxic and p-type semiconductor with excellent electrocatalytic properties, becomes a candidate material for the non-enzymatic glucose sensors [1,2]. Compared with other glucose sensing materials, such as enzymes [3,4], noble metals [5,6], transition metals [7,8], and transition metal oxides [9], CuO exhibits many advantages including excellent stability, low cost, and high reliability [1,10,11]. The past ten years has witnessed growing interest in the design and synthetic approaches for various nanostructured CuO, such as nanofibers [12], nanospheres [13], nanorods [2], and nanowires [14,15]. However, fabrication of CuO based glucose sensors with desirable performance remains a great challenge due to the "trade-off effect" between sensitivity and linear range. As summarized in Figure 1, either high sensitivity [16–20] or wider linear range [2,12–14,21–23] can be obtained independently, however, it is very hard to achieve both at the same time. In general, by exposing more active sites for glucose oxidation improves sensitivity. Nevertheless, it could not maintain wider linear range because of no guarantee for sufficient glucose transfer at higher concentration and vice versa. To address these issues, hierarchical CuO nanostructure with three-dimensional interconnected porous network [24] might be an effective approach to balance the "trade-off effect", since the regulated and interconnected nanosize channels could enable fast glucose transfer under high glucose concentration. Meanwhile, exposing the vast nanostructure CuO features benefits sensitivity by increasing active sites for glucose oxidation.

Recently, nanoporous metal (NPM) fabricated via dealloying [25–28] has attracted great attention, in which active metal elements are selectively dissolved, and a three-dimensional and nanoporous framework is formed by the reorganization of the remaining components. It provides a

*Corresponding author (email: zhaiwei322@nwpu.edu.cn)

© Science China Press and Springer-Verlag GmbH Germany, part of Springer Nature 2020

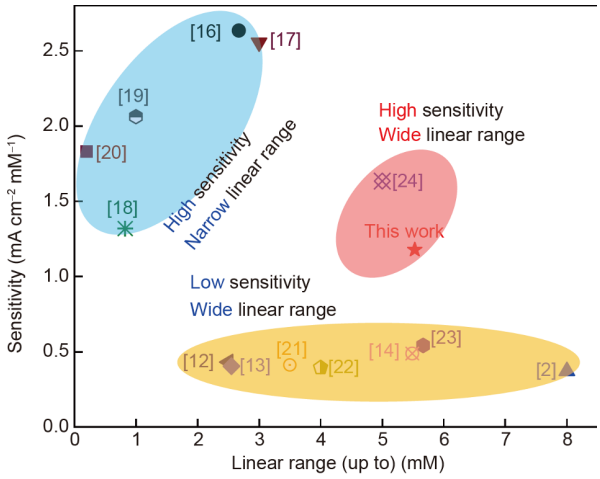

Figure 1 (Color online) Performance comparison of several CuO based electrochemical glucose sensors.

facial approach of preparing metal oxides with nanoporous structure for catalyst and sensing applications. In this study, a hierarchical CuO nanostructure is prepared by dealloying of Al-33.3 wt% Cu eutectic alloy ribbons and consequent oxidation process. The morphological structure of the obtained CuO is carefully investigated. The hierarchical CuO nanostructure shows excellent glucose sensing performance in terms of higher sensitivity and wider linear range.

2 Experimental method

2.1 Materials

Al (purity, 99.999 wt%) and Cu (purity, 99.999 wt%) elements were purchased from China New Metal Materials Technology Co., Ltd.. Ethanol (C_2H_5OH, Tianjin chemical reagent Co., Ltd.), glucose ($C_6H_{12}O_6$, Aladdin Co., Ltd.), sodium hydroxide (NaOH, Tianjin Chemical Reagent Co., Ltd.), ascorbic acid ($C_6H_8O_6$, Aladdin Co., Ltd.), uric acid ($C_5H_4N_4O_3$, Aladdin Co., Ltd.), hydrogen nitrate (HNO_3, Guangdong Guanghua Sci-tech Co., Ltd.) and Nafion solution (0.5 wt% in a mixture of lower aliphatic alcohols and water, Sigma Aldrich) were used as received. All the aqueous solutions were prepared with Milli-Q-filtered water (resistivity at 25°C > 18.18 MΩ cm).

2.2 Preparation and microstructure characterization of hierarchical CuO nanostructure

The Al-33.3 wt% Cu eutectic alloy ribbons with 20–50 μm in thickness and 2–4 mm in width were obtained by using single roller melt spinning technique at a speed of 2600 r min^{-1} under argon atmosphere. The as-spun alloy ribbons were immerged into the NaOH (1 M) aqueous solution at 25°C under continuous N_2 inletting for 1 h to dissolve Al element. Then, the dealloyed sample in NaOH solution underwent pre-oxidation process by inletting O_2 for 3 min. After this, the pre-oxidized sample was removed and washed by dehydrated ethanol and distilled water for three times, and was finally annealed in a furnace at 500°C for 4 h. For comparison, the other two annealed CuO samples (SA1 and SA2) were prepared by controlling pre-oxidation time and washing cycles as shown in Supporting Information. The above mentioned process was schematically illustrated in Figure 2. The crystalline structure of the samples was recorded by X-ray diffraction (XRD, Maxima_X XRD-7000X, Shimadzu, Japan). The morphological microstructures of the samples were determined by field-emission scanning electron microscopy (FE-SEM, Verios G4, FEI, USA).

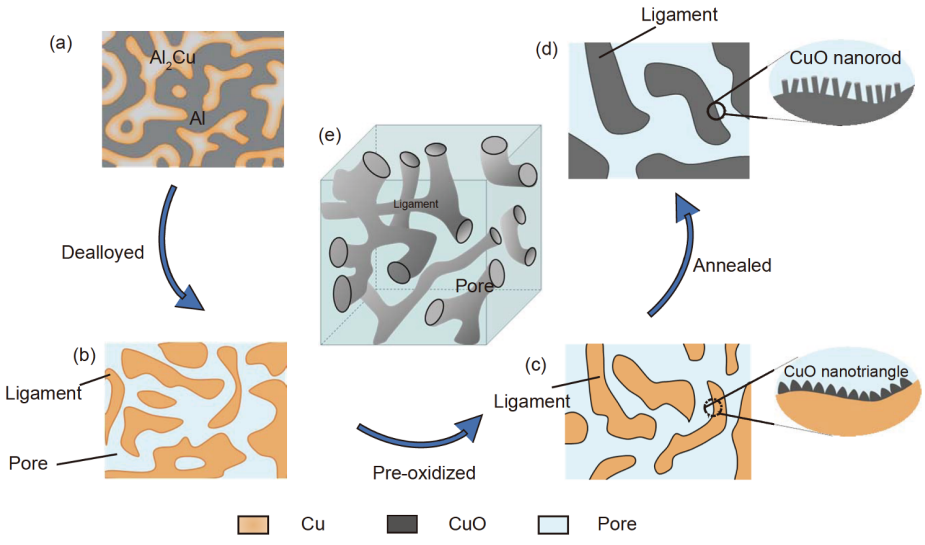

Figure 2 (Color online) Schematic illustration of preparation process and the corresponding microstructure evolution: two-dimensional illustration of (a) Al-33.3 wt% Cu eutectic alloy ribbons (As-spun), (b) dealloyed sample with ligaments and pores, (c) pre-oxidized sample (Pre-oxidized) mixed by Cu and CuO with ligaments and pores, (d) O_2 annealed sample (Annealed) composed of CuO nanostructure, (e) three-dimensional illustration of annealed sample.

2.3 Fabrication of modified electrode and electrochemical measurements

All the electrochemical measurements were carried out by electrochemical station (CHI 660e and Autolab PGSTAT M204). The glass carbon electrode (GCE) with diameter of 3 mm was polished by using 0.3 and 0.05 mm alumina micro-polish paste, and was washed with HNO_3/water mixture (*v*/*v*, 1:1), ethanol, deionized water and dried at room temperature. Then, 7.5 μL CuO ethanol suspension (5 mg mL^{-1}) was dropped onto GCE surface. The CuO@GCE was covered by 2.5 μL of Nafion solution (0.5 wt%) to make sure solid attachment of CuO and dried in air. Electrochemical measurements were performed using a conventional three-electrode cell comprising a CuO@GCE as the working electrode, a platinum plate as a counter electrode and an Ag/AgCl as the reference electrode. The cyclic voltammetry (CV) and amperometric measurement were applied to analyze the glucose sensing performance of the CuO at several scan rates from 10 to 100 mV s^{-1} in a 0.1 M NaOH solution containing of certain amount of glucose. The amperometric response was recorded under a successive addition of stepwise changing glucose concentrations in 0.1 M NaOH solution at 50-s time intervals.

3 Results and discussion

Figure 3 shows the phase constitution and morphology of the as spun, pre-oxidized and annealed samples. Clearly, the as-spun ribbons were composed of Al_2Cu intermetallic compound (JCPDS No.25-0012) and α-Al solid solution (JCPDS No.04-0787), and characterized by the eutectic Al_2Cu phase homogeneously distributed on Al phase. After dealloying and pre-oxidation in the alkali solution, CuO (JCPDS No.48-1548) phase is detected with the coexistence of Cu (JCPDS No.04-0836) phase in the pre-oxidized sample. It is featured by typical bicontinuous and interconnected ligament-channels due to selective dissolution of Al atoms during dealloying. Large amount of triangle nanoflakes are uniformly spread along the ligament surface, which are probable CuO owing to the partial oxidation of Cu after suitable O_2 inletting and washing cycles as shown in Figure 3(c). After O_2 annealing, a transformation to monoclinic CuO (JCPDS No.48-1548) is completed. As shown in Figure 3(d), a hierarchical CuO nanostructure is obtained, in which a large amount of firecracker-shaped CuO nanorods with 20 nm in width and 80 nm in length are homogeneously distributed on the ligaments. In addition, the energy dispersive X-ray spectroscopy (EDS) of annealed sample is provided in Figure 3(g), there is only tiny Al element (around 1% atomic) preserved owing to incomplete dissolving. The above mentioned microstructural evolution is also shown in Figure 2. The pore and ligament size distribution of the pre-oxidized and annealed samples are presented in Figure 3(e) and (f). After annealing, the interconnected nanoporous structure is well preserved with a clear pore enlargement, in which the mean pore size is increased from 100 to 200 nm. Meanwhile, an obvious ligament coarsening is detected by the enhancement of the mean ligament size from 150 to 200 nm due to the active surface diffusion.

To achieve a glucose sensor with excellent performance, the primary task is to understand the electrochemical kinetics during electro-oxidation of glucose. In general, the electrochemical kinetics could be derived from the dependence of current on scanning rate from CV curves. Figure 4(a) presents a continuous increase of the anodic peak current (I_{pa})

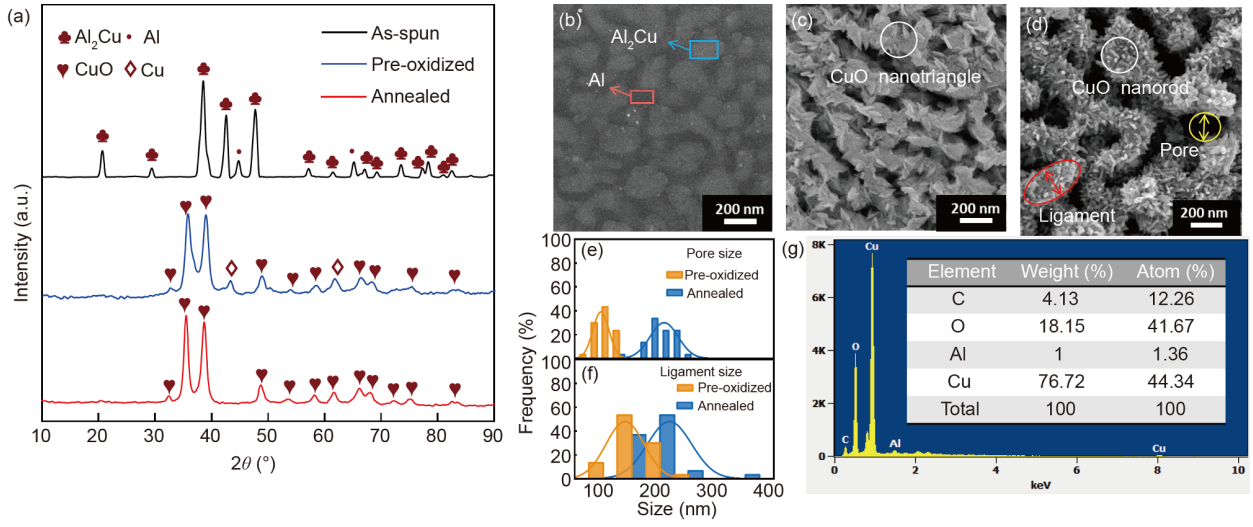

Figure 3 (Color online) Phase constitution and microstructural characterization: (a) XRD patterns of the as-spun, pre-oxidized and annealed samples; SEM images of (b) as-spun sample, (c) pre-oxidized sample and (d) annealed sample; pore and ligament size distribution of (e) pre-oxidized and (f) annealed sample; (g) SEM-EDS analysis of annealed sample (the inset presents element distribution).

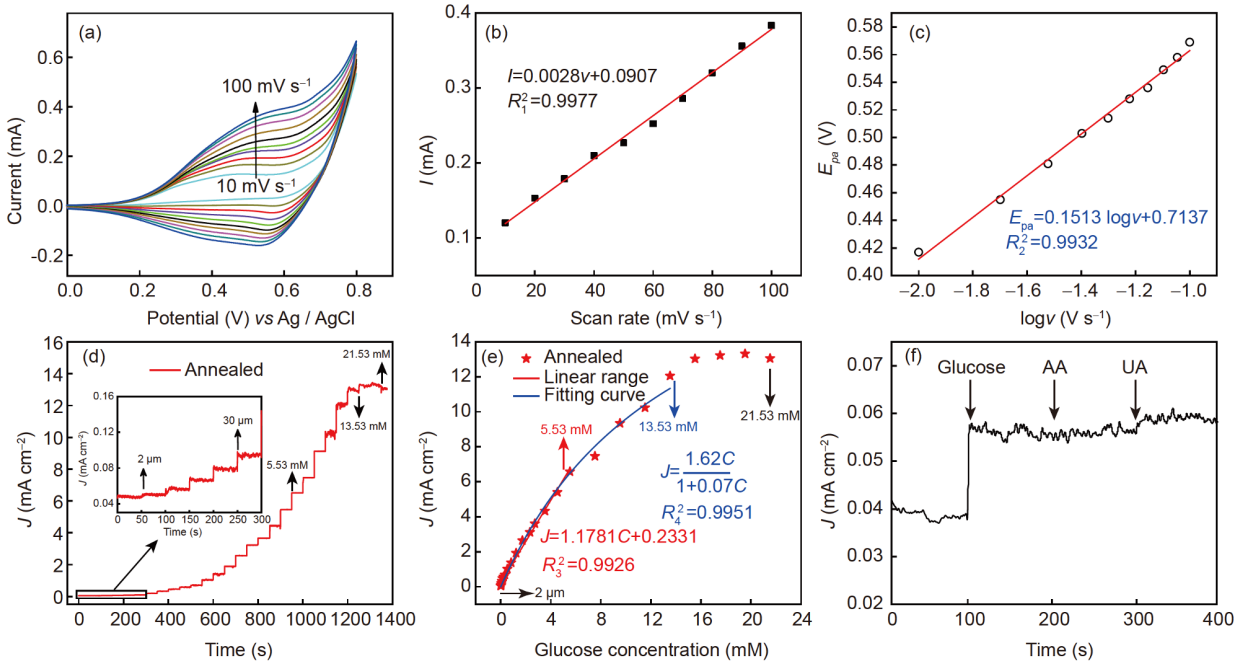

Figure 4 (Color online) Electrochemical kinetics, amperometric response and anti-interference property of CuO@GCE: (a) CV curves at scan rate from 10 to 100 mV s^{-1}; (b) the calibration plot of (a); (c) plot of E_{pa} against the log$v$; (d) amperometric response at 0.55 V with successive addition of glucose (The inset shows respective amperometric response at low concentration level from 2 to 30 μM); (e) calibration plots of (d); (f) amperometric response to injections of 1 mM glucose and 0.1 mM interfering species of AA and UA.

with the increasing of scan rate. Meanwhile, the anodic peak potential (E_{pa}) is shifted to positive direction by increasing scan rate v. As shown in the Figure 4(b), I_{pa} of glucose oxidation shows a linear relationship regressed by I_{pa}(mA) =0.0028v+0.0907 with a correlation coefficient R_1^2 =0.9977. This suggests that the electrocatalytic behavior of glucose on CuO@GCE follows the surface adsorption-controlled process. In the case of diffusionless electrochemical systems, voltammetry method could be used to study the transfer coefficient (α) and the apparent reaction rate constants (k_s) of the catalytic reaction. The transfer coefficient can be calculated by using Laviron's equation [29–31]:

$$E_{pa} = E^j + \frac{2.303RT}{(1-\alpha)nF}\log\frac{(1-\alpha)nF}{RTk_s} + \frac{2.303RT}{(1-\alpha)nF}\log v, \quad (1)$$

where E_{pa} is the anode peak potential (V), E^j is equal to the surface standard potential (V), v is the scan rate (V s^{-1}), n is number of electrons involved (assumed to be 1), F is the Faraday constant, R is the gas constant, and T is the temperature. Figure 4(c) shows the linear relationship of the E_{pa} and log$v$, in which the linear regression equation is E_{pa}= 0.1513log$v$+0.7137 (R_2^2=0.9932). Therefore, α can be easily calculated to be 0.6. And the k_s can be obtained as 0.18 s^{-1} from the following equation, which is higher than that of other two CuO samples (shown in Figure S3 in Supporting Information).

$$\log k_s = \alpha\log(1-\alpha) + (1-\alpha)\log\alpha - \log\frac{RT}{nFv} - \frac{\alpha(1-\alpha)nF\Delta E_p}{2.303RT}. \quad (2)$$

For further determining sensitivity and linear range of CuO@GCE, a stair-like tendency of amperometric response is detected by an addition of step-wise changing glucose concentrations in Figure 4(d). As shown in the inset, a slight increase in current response is pointed out by an initial addition of 2 μM glucose, presenting the current response of CuO@GCE under low concentration of glucose ranging from 2 to 30 μM. Then, a stepwise increase in current response appears with the addition of glucose concentration range from 30 μM to 21.53 mM. Finally, the corresponding calibration curve between current response and glucose concentration is plotted in Figure 4(e). The linear regression could be expressed by the following equation:

$$J\ (\text{mA cm}^{-2}) = 1.1781\ C\ (\text{mM}) + 0.2331, \quad R_3^2 = 0.9926, \quad (3)$$

where J and C represent the current density and glucose concentration, respectively. According to linear regression equation, the sensitivity for annealed CuO is about 1.18 mA cm^{-2} mM^{-1}, and linear range is up to 5.53 mM with a lower detection limit of 0.40 μM (S/N=3). Comparing the other glucose sensing performance summarized in Figure 1, the "trade-off effect" is well balanced, and both high sensi-

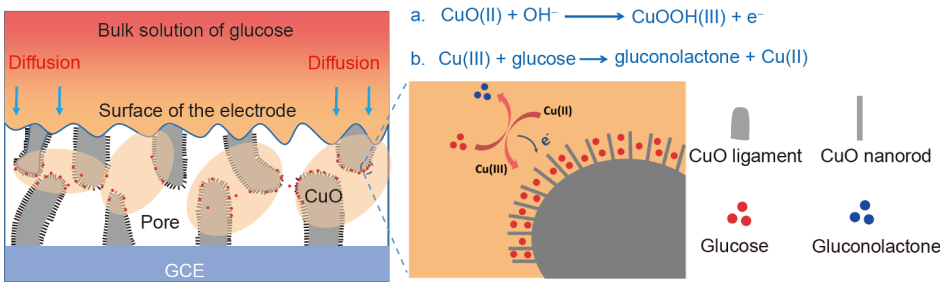

Figure 5 (Color online) Mechanism of electro-oxidation of glucose at hierarchical nanoporous CuO modified GCE.

tively and wide linear range are achieved in specific hierarchical CuO nanostructure.

Furthermore, the glucose oxidation over hierarchical nanostructured CuO follows the surface adsorption-controlled process. Thus Langmuir adsorption isotherm equation [32] can be used to describe the concentration of glucose adsorbed on the catalyst surface (C_s):

$$C_s = \frac{K_A C_{glucose} C_t}{1 + K_A C_{glucose}}, \tag{4}$$

where K_A is the adsorption equilibrium constant, $C_{glucose}$ is concentration of glucose in the bulk solution, C_t is the constant, which means the total molar concentration of active sites on CuO. And under a given potential, current density (J) is proportional to C_s with a rate constant of K_B, thus the relationship of the J and C_s can be expressed with the following equation [33]:

$$J = K_B C_s = \frac{K_A K_B C_{glucose} C_t}{1 + K_A C_{glucose}} = \frac{K C_{glucose}}{1 + K_A C_{glucose}}, \tag{5}$$

where K is $K_A K_B$. As shown in Figure 4(e), the calibration fitting equation can be expressed as follows:

$$J = \frac{1.62C}{1 + 0.07C}, \quad R_4^2 = 0.9951. \tag{6}$$

According to the fitting, a wider dynamic range of glucose oxidation (0.002–13.53 mM) is achieved.

In addition, anti-interference is another important parameter to consider, because many co-existing electroactive species such as ascorbic acid (AA) and uric acid (UA) in the real blood sample might cause disturbing signals. The amperometric *I-t* test based on CuO@GCE with two different interfering species are carried out in the supporting electrolyte containing 0.1 M NaOH. The concentration of the interfering species is fixed 1/10 of the glucose despite their actual lower ratio (1/40 to 1/30) to glucose in human blood. As shown in Figure 4(f), a significant and steady current increase is detected while 1 mM glucose is added to the solution. Interfering signals are only 1.7% for AA and 5.9% for UA in comparison with glucose, indicating strong anti-interference capability of present glucose sensor.

The mechanism for improving glucose electro-oxidation by optimizing micro-environment is illustrated in Figure 5. With the presence of glucose in alkaline solution, previous oxidized Cu (III) is served as active oxidant to react with adsorbed glucose to form gluconolactone and is reduced to Cu (II), resulting in J_{pa} at 0.55 V. Generally, the electro-oxidation of glucose is highly depended on the nanostructure of CuO. By comparing the apparent constant of reaction (k_s) of CuO with different morphology (Figure S3), the kinetics of glucose oxidation process is highly enhanced due to hieratical nanostructure. On the one hand, a great number of firecracker-shaped CuO nanorods provide high sensitivity by increasing the surface area (Figure S2) and the number of active sites for glucose's electro-oxidation. On the other hand, porous structure is proven to be responsible for mass transport [34], thus the nanosized interconnected porous structure enable a wider linear range through accelerating glucose transfer under high concentration. This indicates that hierarchical CuO nanostructure with massive nanorods acts as excellent candidate for glucose sensing material.

4 Conclusion

In summary, the hierarchical CuO nanostructure consisting of bicontinuous ligaments along with vast of firecracker-shaped nanorods and three-dimensional interconnected nanoporous channels is fabricated through properly controlling the dealloying and post-oxidation process of Al-33.3 wt% Cu eutectic alloy ribbons. The CuO based glucose sensor presents a high sensitivity of 1178.1 μA cm^{-2} mM^{-1} in a wider linear range from 2 μM to 5.53 mM. The unique hierarchical nanostructure not only enhances the number of active cites of glucose oxidation but also accelerates glucose transfer, finally balancing the "trade-off" effect between sensitivity and linear range. This work provides a facile method to fabricate metal oxide with hierarchical nanostructure and desirable electrocatalytic properties.

The authors thank Prof. B. Wei who provided insights and expertise that greatly assisted the research, and thank Dr. Y Meng for the valuable dis-

cussion of the electrochemical characterization. This work was supported by the National Natural Science Foundation of China (Grant Nos. 51922089, 51972275 and 51727803), Science and Technology Coordination Innovation Project in Shaanxi Province (Grant No. 2019KW-024), and Fundamental Research Funds for the Central Universities (Grant No. 310201911fz050).

Supporting Information

The supporting information is available online at tech.scichina.com and link.springer.com. The supporting materials are published as submitted, without typesetting or editing. The responsibility for scientific accuracy and content remains entirely with the authors.

1 Zhang Q, Zhang K, Xu D, et al. CuO nanostructures: Synthesis, characterization, growth mechanisms, fundamental properties, and applications. Prog Mater Sci, 2014, 60: 208–337
2 Wang X, Hu C, Liu H, et al. Synthesis of CuO nanostructures and their application for nonenzymatic glucose sensing. Sens Actuat B-Chem, 2010, 144: 220–225
3 Hui Y, Ma X, Qu F, et al. Three-dimensional nickel foam based enzymatic electrode and its glucose/O_2 biofuel cell with high power density. J Electrochem Soc, 2017, 164: G112–G120
4 Campbell A S, Islam M F, Russell A J. Intramolecular electron transfer through poly-ferrocenyl glucose oxidase conjugates to carbon electrodes: 1. Sensor sensitivity, selectivity and longevity. Electrochim Acta, 2017, 248: 578–584
5 Li Y, Niu X, Tang J, et al. A comparative study of nonenzymatic electrochemical glucose sensors based on Pt-Pd nanotube and nanowire arrays. Electrochim Acta, 2014, 130: 1–8
6 He B, Hong L, Lu J, et al. A novel amperometric glucose sensor based on PtIr nanoparticles uniformly dispersed on carbon nanotubes. Electrochim Acta, 2013, 91: 353–360
7 Darvishi S, Souissi M, Karimzadeh F, et al. Ni nanoparticle-decorated reduced graphene oxide for non-enzymatic glucose sensing: An experimental and modeling study. Electrochim Acta, 2017, 240: 388–398
8 Ma P, Ma X, Suo Q, et al. Cu NPs@NiF electrode preparation by rapid one-step electrodeposition and its sensing performance for glucose. Sens Actuat B-Chem, 2019, 292: 203–209
9 Ci S, Huang T, Wen Z, et al. Nickel oxide hollow microsphere for non-enzyme glucose detection. Biosens Bioelectron, 2014, 54: 251–257
10 Chen F, Cao Q, Dong C, et al. Ultrasonic polymerization of CuO@PNIPAM and its temperature tuning glucose sensing behavior. Ultrason Sonochem, 2018, 49: 190–195
11 Liu Z, Bando Y. A novel method for preparing copper nanorods and nanowires. Adv Mater, 2003, 15: 303–305
12 Wang W, Zhang L, Tong S, et al. Three-dimensional network films of electrospun copper oxide nanofibers for glucose determination. Biosens Bioelectron, 2009, 25: 708–714
13 Reitz E, Jia W, Gentile M, et al. CuO nanospheres based nonenzymatic glucose sensor. Electroanalysis, 2008, 20: 2482–2486
14 Zhang P, Zhang L, Zhao G, et al. A highly sensitive nonenzymatic glucose sensor based on CuO nanowires. Microchim Acta, 2012, 176: 411–417
15 Zhang Y, Liu Y, Su L, et al. CuO nanowires based sensitive and selective non-enzymatic glucose detection. Sens Actuat B-Chem, 2014, 191: 86–93
16 Wang X, Ge C, Chen K, et al. An ultrasensitive non-enzymatic glucose sensors based on controlled petal-like CuO nanostructure. Electrochim Acta, 2018, 259: 225–232
17 Zhang X, Sun S, Lv J, et al. Nanoparticle-aggregated CuO nanoellipsoids for high-performance non-enzymatic glucose detection. J Mater Chem A, 2014, 2: 10073
18 Chakraborty P, Dhar S, Debnath K, et al. Glucose and hydrogen peroxide dual-mode electrochemical sensing using hydrothermally grown Cuo nanorods. J Electroanal Chem, 2019, 833: 213–220
19 Ashok A, Kumar A, Tarlochan F. Highly efficient nonenzymatic glucose sensors based on CuO nanoparticles. Appl Surf Sci, 2019, 481: 712–722
20 Chawla M, Sharma V, Randhawa J K. Facile one pot synthesis of CuO nanostructures and their effect on nonenzymatic glucose biosensing. Electrocatalysis, 2017, 8: 27–35
21 Sahoo R K, Das A, Samantaray K, et al. Electrochemical glucose sensing characteristics of two-dimensional faceted and non-faceted CuO nanoribbons. CrystEngComm, 2019, 21: 1607–1616
22 Liu X, Yang Y, Liu R, et al. Synthesis of porous CuO microspheres assembled from (001) facet-exposed nanocrystals with excellent glucose-sensing performance. J Alloys Compd, 2017, 718: 304–310
23 Yang P, Wang X, Ge C, et al. Fabrication of CuO nanosheets-built microtubes via Kirkendall effect for non-enzymatic glucose sensor. Appl Surf Sci, 2019, 494: 484–491
24 Sun S, Zhang X, Sun Y, et al. A facile strategy for the synthesis of hierarchical CuO nanourchins and their application as non-enzymatic glucose sensors. RSC Adv, 2013, 3: 13712–13719
25 Xu C, Wang R, Zhang Y, et al. A general corrosion route to nanostructured metal oxides. Nanoscale, 2010, 2: 906–909
26 Kim Y T, Lopes P P, Park S A, et al. Balancing activity, stability and conductivity of nanoporous core-shell iridium/iridium oxide oxygen evolution catalysts. Nat Commun, 2017, 8: 1449
27 Dong C, Kou T, Gao H, et al. Eutectic-derived mesoporous Ni-Fe-O nanowire network catalyzing oxygen evolution and overall water splitting. Adv Energy Mater, 2018, 8: 1701347
28 Li R, Liu X, Wang H, et al. Sandwich nanoporous framework decorated with vertical CuO nanowire arrays for electrochemical glucose sensing. Electrochim Acta, 2019, 299: 470–478
29 Laviron E. General expression of the linear potential sweep voltammogram in the case of diffusionless electrochemical systems. J Electroanal Chem, 1979, 101: 19–28
30 Laviron E. The use of linear potential sweep voltammetry and of a.c. voltammetry for the study of the surface electrochemical reaction of strongly adsorbed systems and of redox modified electrodes. J Electroanal Chem, 1979, 100: 263–270
31 Wang M F, Huang Q A, Li X Z, et al. Mesoporous CuO: Alternative enzyme-free glucose sensing structure with excellent kinetics of electrode process. Anal Methods, 2012, 4: 3174–3179
32 Fogler H S. Elements of chemical reaction engineering. Chem Eng Sci, 1987, 42: 2493
33 Ding Y, Wang Y, Su L, et al. Electrospun Co_3O_4 nanofibers for sensitive and selective glucose detection. Biosens Bioelectron, 2010, 26: 542–548
34 Liang T, Zou L, Guo X, et al. Rising mesopores to realize direct electrochemistry of glucose oxidase toward highly sensitive detection of glucose. Adv Funct Mater, 2019, 29: 1903026